agronomy

MDPI

Article

A Characterization of the Functions of OsCSN1 in the Control of Sheath Elongation and Height in Rice Plants under Red Light

Shining Han [1,†], Yanxi Liu [1,†], Anor Bao [1], Tongtong Jiao [1], Hua Zeng [1], Weijie Yue [1], Le Yin [1], Miao Xu [1], Jingmei Lu [2], Ming Wu [1,*] and Liquan Guo [1,*]

[1] College of Life Sciences, Jilin Agricultural University, Changchun 130118, China; hhshining@163.com (S.H.); lyx309660408@163.com (Y.L.); 15047535821@163.com (A.B.); jtt1163933169@163.com (T.J.); 18670148531@163.com (H.Z.); 13173433829@163.com (W.Y.); lyjiau@126.com (L.Y.); miaox@jlau.edu.cn (M.X.)
[2] School of Life Sciences, Northeast Normal University, Changchun 130024, China; jingmlu@163.com
* Correspondence: mingw@jlau.edu.cn (M.W.); guolq948@nenu.edu.cn (L.G.)
† These authors contributed equally to this work.

Abstract: The COP9 signalosome (CSN) is a conserved protein complex, with CSN1 being one of the largest and most important subunits in the COP9 complex. To investigate the N-terminus function of OsCSN1, we edited the N-terminus of OsCSN1 and found that the mutant of OsCSN1 with 102 amino acids missing at the N-terminus showed insensitivity to red light in terms of the embryonic sheath, stem elongation, and main-root elongation. Moreover, the mutant was able to produce, develop, and bear fruit normally. The research results indicate that OsCSN1 is a negative regulator of stem elongation in rice seedlings regulated by red light. Under red-light treatment, OsCSN1 assembles into CSN, which degrades SLR1 through de NEDDylation, affecting PIL11 activity and ultimately inhibiting stem elongation. OsCSN1 also plays an important regulatory role in the inhibition of rice embryonic sheath elongation under red light. By regulating the degradation of SLR1 and PIL14 through the ubiquitin/26S protease pathway, the elongation of the embryonic sheath is ultimately inhibited. OsCSN1 forms a COP9 complex and is modified with RUB/NEDD8 of the E3 ligase of CUL1 to promote the degradation of SLR1 and PIL14, ultimately affecting the elongation of the embryonic sheath. The regulatory domain is located at the N-terminus of CSN1.

Keywords: COP9 signalosome (CSN); rice (*Oryza sativa* L. spp. *japonica*); red light; ubiquitin degradation; hormone

Citation: Han, S.; Liu, Y.; Bao, A.; Jiao, T.; Zeng, H.; Yue, W.; Yin, L.; Xu, M.; Lu, J.; Wu, M.; et al. A Characterization of the Functions of OsCSN1 in the Control of Sheath Elongation and Height in Rice Plants under Red Light. *Agronomy* **2024**, *14*, 572. https://doi.org/10.3390/agronomy14030572

Academic Editors: Sang-Won Lee and Houcheng Liu

Received: 29 January 2024
Revised: 27 February 2024
Accepted: 11 March 2024
Published: 13 March 2024

1. Introduction

The COP9 signalosome (CSN) is a conserved protein complex that is usually composed of eight subunits (named CSN1 to CSN8) in higher eukaryotes (such as plants and animals). However, CSN is a conserved protein complex in some low-level eukaryotes, such as plants and animals. Eukaryotes (such as yeast) are composed of fewer subunits. CSN was first identified in *Arabidopsis* as an inhibitor of photomorphogenesis. It was later considered a 450-kDa nuclear-enriched protein complex ubiquitous in almost all eukaryotes with conserved structures [1–3]. Biochemical, genetic, and genomic studies have shown that CSN regulates various cellular processes, including cell-cycle progression, signal transduction, and transcriptional regulation [1–3].

CSN has recently been shown to interact with Skp1-cullinF-box (SCF) E3 ubiquitin ligases and promote the Rub1/Nedd8 deconjugation of the SCF cullin subunit [4,5]. SCF represents a conserved class of E3 enzymes that contain Skp1, Cdc53/cullin, and Hrt1/Roc1/Rbx1 as core components [6]. Rub1/Nedd8 is a ubiquitin-related polypeptide that can be conjugated to members of the Cullin family through an enzymatic cascade similar to that of ubiquitin conjugation [7,8]. Cullin modification is necessary for the proper function of SCF in higher eukaryotes [9].

Plants sense signals, such as differences in light quality and intensity, and constantly adjust their growth and development to adapt to the changing environment to the greatest extent possible. Numerous studies have shown that light affects multiple developmental processes in plants, from seed germination to fruit maturity [10,11]. Plants complete this critical task using a series of photoreceptors, such as phytochromes (phy), cryptochromes, and phototropins. The phy family mainly senses and responds to red (R) and far-red (FR) light regions and controls various responses in the plant life cycle. A small gene family encodes phytochromes in higher plants, and the phytochrome gene family in Arabidopsis consists of five members (PHYA~PHYE) [12,13]. The rice phytochrome gene family includes three members: PHYA, PHYB, and PHYC [14–17].

Different monochromatic lights can affect plant growth and quality by regulating photosynthesis, photomorphogenesis, and secondary metabolism [18–20]. Phytochromes play a wide range of roles in plant responses to red and far-red light [21,22]. Studies have shown that, compared with white light, red light can cause a reduction in plant biomass and leaf area [23–26], cause excessive stem elongation, and affect leaf number and chlorophyll content [18,27]. The adverse effects caused by monochromatic red light, the so-called "red light syndrome" [28], are mainly due to the stimulation of phytochromes by the lack of far-red light, resulting in an imbalance of phytochromes [29]. Overall, impaired plant growth results from the effect of red light on plant photosynthesis, which is caused by a sluggish stomatal response, low photosynthetic capacity, and low utilization efficiency [30–32]. Additionally, in the presence of red light, phyB undergoes a conformational change from the red light-absorbing form (Pr) to the far-red light-absorbing form (Pfr), resulting in a blocked light-absorbing form (Pfr). The receptive area is exposed, thereby causing the nuclear translocation of phyB [33]. Previous studies have shown that phyB is essential in regulating de-etiolation, leaf angle, flowering stage, and abiotic stress responses in rice seedlings. phyB can sense red light and positively regulate chlorophyll synthesis in rice, whereas red light inhibits coleoptile elongation in seedlings and plays a significant role in this process [34].

Light signals can affect plant hormone metabolism and responses, and hormone status can also affect plant responses to light [35–37]. As a diterpene phytohormone, gibberellins (GAs) are critical regulatory hormones in plant growth and development and affect many aspects of plants' seed germination, stem and leaf growth, and flower and fruit development. Among them, GA has the most vigorous physiological activity and has been studied the most; the most common GA is GA3 [38,39]. Studies on *Arabidopsis thaliana* revealed that the DELLA protein is a negative regulator of the GA-signaling pathway. There are five DELLA proteins in *Arabidopsis* [40], but only one DELLA protein, SLENDER RICE1 (SLR1), has been found in rice. Because the GA-signaling mechanism is conserved, SLR1 is a negative regulator of the GA-signaling pathway in rice [41]. Arizumi et al. [42] reported that the inhibition of Arabidopsis seed germination via DELLA could be alleviated by proteolysis via the ubiquitin–proteasome pathway or by GA hormone signaling in a proteolysis-independent manner. The binding of GA to the GA receptor GID1 stimulates the formation of the GID1-GA-DELLA complex, which in turn triggers the ubiquitination and proteolysis of the DELLA protein through the SCF (SLY1) E3 ubiquitin ligase and the 26S protease receptor.

Under normal light conditions, light can induce photomorphogenesis in plants. Phytochromes sense red or far-red lights. In plants, the phytochrome exists in the cytoplasm in an inactive Pr conformation. When a plant is irradiated with light, phytochrome molecules are converted into a biologically active Pfr conformation. The phytochrome in the Pfr form is transferred to the nucleus [43], where it interacts with phytochrome-interacting factors (PIFs) to induce the expression of light-regulated genes and photomorphogenesis [44,45]. However, as mentioned above, GA inhibits photomorphogenesis, which is the opposite of the effect of light. Recently, the molecular mechanisms underlying the antagonistic effects of GA and phytochromes on the regulation of photomorphogenesis in Arabidopsis have been reported [46–48]. The phyB-signaling mechanism also involves direct interactions with

COP1, a RING-finger E3 ubiquitin ligase that negatively regulates photomorphogenesis and its enhancer, SPA1 [49].

The role of the CSN complex in regulating the growth and development of organisms has received increasing attention. Studies have shown that Arabidopsis CSN1 requires the integrity of the CSN complex to maintain its stability in CSN1 plants. The PCI domain of CSN1 is involved in interactions between complex subunits and plays a critical role in complex formation. On the other hand, the N-terminus of CSN1 was not involved in the formation of the CSN complex but had other essential functions that are still unclear. In particular, the role of CSN1 in rice has yet to be determined. Therefore, this study used gene editing and overexpression technology to construct and screen OsCSN1-knockout and -overexpression mutants in rice (*Oryza sativa* L. spp. *japonica*). Phenotypic changes in the mutants were observed under red-light conditions, and phenotypic and proteomic changes in the mutants were analyzed through the addition of the exogenous hormone GA and the GA-synthesis inhibitor paclobutrazol (PAC) to investigate the mechanisms of OsCSN1-related germination. The location of OsCSN1 expression in rice seedlings under different treatments was spatiotemporally analyzed. Considering the changes in the expression levels of hormone-related proteins in rice seedlings under different light treatments, it was speculated that the expression levels of OsCSN1 in rice seedlings under different light treatments were significantly different from the expression levels of OsCSN1 in rice seedlings under red-light and hormone treatments and the signaling pathways for seedling growth and biological function of the N-terminus of OsCSN1. Through this pathway, the growth of rice seedlings can be promoted by adjusting light and hormone treatments, thereby shortening the growth cycle and having a certain impact on improving the agronomic traits of rice.

2. Materials and Methods

2.1. Protein Structure Prediction

After searching for protein sequences on NCBI, we used DNAMAN, the Expasy website, Plant mP Loc, NetPhos 3.1 Server, PSIPRED Workbench, and SWISS MODLE to compare analysis sequences, analyze the primary structure, predict the subcellular localization, and predict the phosphorylation site and the tertiary structure of the OsCSN1 protein.

2.2. Construction of Plant Expression Vectors and Screening of Mutant Strains

In this study, rice was used as a wild-type control and knockout and overexpression mutants were constructed. We searched and amplified the sequences of rice (*Oryza sativa* L. spp. *japonica*) on NCBI. Three gRNA targets were designed on Exon1 of OsCSN1 using CRISPR/Cas9 gene-editing technology. The vector, Pp1C.3 (containing the OsU3 promoter), suitable for monocotyledonous plants, was selected, and OsCSN1 single-gene knockout vectors OsCSN1G1, OsCSN1G2, and OsCSN1G3 were constructed using the homologous recombination principle. To construct the overexpression vector, pCUbi1390 was selected. OsCSN1 full length, the OsCSN fragment without N-terminal 32 amino acid (amino acid 33-441) (OsCSN1DN32) length, the CSN fragment without N-terminal 102 amino acid (amino acid 103-441) (OsCSN1DN102) length, and GFP length were amplified separately. The amplified sequence was connected to the cleaved pCUbi1390 plasmid through multi-fragment homologous recombination. OsCSN1-GFP, OsCSN1DN32-GFP, and OsCSN1DN102-GFP constructed vectors were obtained, respectively. We transferred the constructed knockout and overexpression vectors into rice using a Agrobacterium-mediated method. The cultivation and passage of rice through callus tissue after PCR and Western Blot experiments, and OsCSN1 knockout mutants and reduce mutants oscsn1-1 and oscsn1-2 were screened, as well as the OsCSN1 entire sequence overexpression mutant strains OsCSN1-GFP-OE, OsCSN1 N-terminal deletant mutant, OsCSN1DN32-GFP-OE, and OsCSN1DN102-GFP-OE mutant.

2.3. Growth Conditions and Data Measurement of Plant Materials

The husks were removed from rice seeds, soaked in 75% ethanol for 5–10 min, disinfected with Bleach made of 70% NaCIO and 1% X-Triton for 30 min, removed from Bleach, washed 5–6 times with sterile distilled water, and sowed in 0.8% (*w*/*v*) agar medium for cultivation. We added 10 mM/L GA3 and 100 mM/L PAC to the agar medium for hormone treatment. We sowed WT and mutant seeds in the culture medium as mentioned above under red-light treatment conditions of 28 °C and continuous red-light irradiation for 24 h with a wavelength of 650 nm; light treatment at 28 °C, 12 L:12 D light cultivation, light intensity of 24,000 Lx; dark treatment at 28 °C and 24 h cultivation without light.

After 9 days of growth, the WT and samples were measured for plant height, root length, and embryonic sheath length during the seedling stage. All measurements in each group were repeated 5 times (N = 5). Data are presented as mean ± standard error for the control and experimental groups. Statistical significance was set at $p \leq 0.05$. Experimental data were analyzed using Excel 2019 and Statistical Product Service Solutions 28.0 (SPSS, https://www.ibm.com/cn-zh/products/spss-statistics, accessed on 25 May 2023), and graphs were plotted using GraphPad Prism 8 (https://www.graphpad-prism.cn/, accessed on 25 May 2023).

2.4. Protein Extraction and Western Blot/Antibody Analysis

Samples of 0.5 g of 9-day seedlings from the treatment groups mentioned above were frozen in liquid nitrogen and ground. Plant RIPA Lysis Buffer (Beyotime, Shanghai, China) was used to extract proteins from the sample tissue, and a final concentration of 1 mM PMSF was added before use. After thoroughly mixing the sample and extraction solution at a low temperature, the samples were centrifuged at 4 °C and 15,000 rpm for 10 min. The supernatant was transferred to a new tube, and an appropriate amount of sample buffer 5 was added to each sample × Mix SDS-PAGE (Genstar, Beijing, China). The mixed sample was boiled for 10 min and cooled on ice for later use. Protein electrophoresis was performed using 5% concentrated gel and 8% separation gel, with 20 samples per sample μL, and electrophoresis was stopped when the bromophenol blue in the sample reached the bottom of the separation gel using a constant current of 20 mA. The SDS-PAGE gel was transferred onto the PVDF membrane using the Trans-Blot Turbo Blotting System (170-4150, BIO-RAD, Hercules, CA, USA) under a condition of 2.5 V constant pressure for 10 min, sealed with 4% skimmed milk, incubated with the antibody, and then ECL chemiluminescence color developing solution was used for color development (ABclonal, Wuhan, China). The antibodies used in this study were all purchased from Wuhan ABclonal Biotechnology Co., Ltd., including rabbit polyclonal antibody OsphyB, rabbit polyclonal antibody OsCSN2, rabbit polyclonal antibody OsABI5, rabbit polyclonal antibody OsSLR1, rabbit polyclonal antibody OsCUL4, anti-plant action, secondary antibody IgG HRP go anti-rabbit antibody y, and secondary antibody IgG HRP go anti-mouse antibody Use Universal Hood III (731BR03292, BIO-RAD) to visualize the signal.

2.5. Spatiotemporal Positioning

Seal leaves, roots, and embryonic sheaths of rice seedlings were cultured for 9 days on two layers of cover glass slides (24 mm × 60 mm). Images were obtained using a Leica TCS SP8 CARS confocal microscope (Leica, Wetzlar, Germany). Select 10 × 0.40 eyepiece and 20× and observe with an objective lens of 0.70. The selected positioning point was excited with a 488 nm laser and we detected GFP fluorescence with a 500–530 nm band.

2.6. Total RNA Extraction and Real-Time Quantitative Polymerase Chain Reaction

A Spectrum Plant Total RNA kit (Sigma-Aldrich, Darmstadt, Germany) extracted total RNA from the seedlings. Reverse transcription was performed using StarScript II First Strand cDNA Synthetic Mix and gDNA Remover (GenStar, Beijing, China), using total RNA 0.5 mg as a template. A 2x RealStar Green Fast Mixture with ROX (GenStar, Beijing, China) was used to complete a rapid quantitative polymerase chain reaction on a StepOnePlusTM

real-time PCR device (Applied Biosystems, Thermo Fisher Scientific, Waltham, MA, USA). The blank control (rice) *GAPDH* gene (JN848809) was used to quantify relative mRNA levels by averaging three replicates.

3. Results

3.1. The Absence of the Ubiquitination Site at the N-Terminus of OsCSN1 Affected the Deubiquitination of CSN

The NCBI website was searched for rice CSN1 (LOC4331403), located at positions 935098-939209 on chromosome 3. The gene was 4112 bp in length and contained six exons. The full length of the CDS was 1326 bp, encoding a total of 441 amino acids. The molecular weight of the protein was 49,829.76, the total number of atoms was 7004, and the theoretical isoelectric point was 6.42. The average hydrophilicity of the proteins was −0.311, and the aliphatic amino acid index was 91.2. OsCSN1 and AtCSN1 are highly homologous. Previous studies on *Arabidopsis thaliana* showed that the N-terminus of CSN1 is redundant and may have other functions; therefore, the N-terminus of OsCSN1 was selected and removed. In total, 32 amino acids (OsCSN1DN32) and 102 amino acids (OsCSN1DN102) were identified, and their N-terminal functions are further discussed. Compared to those in OsCSN1, the number of standard amino acid residues constituting the active centers of the enzymes in OsCSN1DN32 and OsCSN1DN102 was lower. A comparison of the stability factors of the three proteins revealed that they were stable. However, their half-lives were significantly different in different species of cells, which might be related to the cellular environment and changes in the protein folding structure.

From the perspective of amino acids, the OsCSN1 protein accounted for the highest proportion of nonpolar R-based amino acids (41.8%), whereas acidic amino acids accounted for the lowest proportion (13.4%). The amino acid compositions of OsCSN1DN32 and OsCSN1DN102 were similar to that of OsCSN1, with nonpolar R-group amino acids accounting for the highest proportion (40.5% and 40.4%, respectively) and acidic amino acids accounting for the lowest proportion (13.0% and 12.4%, respectively) (Table 1).

Table 1. Comparison of physicochemical properties of CSN1 among different species.

		Arabidopsis thaliala	***Oryza sativa***	**OsCSN1DN32-OE**	**OsCSN1DN102-OE**
Number of amino acids		441	441	409	339
Molecular weight		50,578.88	49,829.76	46,883.57	38,869.38
Theoretical pI		6.9	6.42	8.16	8.24
Aliphatic index		87.44	91.2	92.35	92.68
Grand average of hydropathicity (GRAVY)		−0.408	−0.311	−0.347	−0.341
Total number of negatively charged residues (Asp + Glu)		60	59	53	42
Total number of positively charged residues (Arg + Lys)		59	55	55	44
Extinction coefficients	assuming all pairs of Cys residues form cystines	37,290	34,060	34,060	28,100
	assuming all Cys residues are reduced	36,790	33,810	33,810	27,850
Estimated half-life	mammalian reticulocytes, *in vitro*	30 h	30 h	0.8 h	1.1 h
	yeast, *in vivo*	>20 h	>20 h	10 min	3 min
	Escherichia coli, *in vivo*	>10 h	>10 h	10 h	>10 h
Instability index		35.41	31.97	29.31	30.74

The secondary structure of OsCSN1 was predicted using the PSIPRED Workbench. We found that, compared with those of AtCSN1, both genes started with random coils and α-helices at the N-terminus, but the difference was that the α-helix of Arabidopsis was shorter and lacked six amino acids compared with that of rice (Figure 1A). OsCSN1 ends with a β-sheet and a random coil at the C-terminus, whereas AtCSN1 does not have the final β-sheet.

The functions of the CSN1 protein in Arabidopsis and rice are different, possibly because of differences in their secondary structures. The N-terminal fragment (amino acid 1-32) contained one α-helix, and the N-terminal fragment (amino acid 1-102) contained five α-helices. Since the α-helix is one of the primary forms of protein secondary structure, and because the biological activity and physicochemical properties of proteins are determined mainly by the integrity of the steric structure, the absence of an α-helix may affect the folding and coiling of the entire protein polypeptide chain. Therefore, the spatial structure of a protein may change as a function of the protein.

Using SWISS MODLE, the tertiary structures of OsCSN1, OsCSN1DN32, and OsCSN1DN102 were predicted (Figure 1B–D). A structural comparison showed that the structures of AtCSN1 and OsCSN1 were generally similar. However, the tail of the entire structure was slightly different due to the addition of an extra β-sheet to OsCSN1. OsCSN1DN32 lacks 32 amino acids in the N segment and contains an α-helix; therefore, this gene is structurally related to the small segment of OsCSN1, but the overall conformation does not change significantly. In contrast, OsCSN1DN102 had a deletion of 102 amino acids at the N-terminus, which significantly impacted the entire structure of CSN1 and significantly differed from the original structure of OsCSN1. This may have resulted in significant changes in the functions of OsCSNDN102, OsCSN1, and OsCSN1DN32.

The iRice-MS platform predicted possible ubiquitination sites in the OsCSN1 protein (Figure 1A). There were 25 lysine ubiquitination sites in the secondary structure of OsCSN1. The possibility of lysine ubiquitination at positions 77, 91, 99, and 215 in rice CSN1 is high (>80%). All phosphorylation sites were less than 80%. The possibility of ubiquitination at positions 77 and 91 is high. Therefore, we speculated that after editing the N-terminus of OsCSN1, the absence of 32 amino acids would not affect the ubiquitination function of OsCSN1. However, after deleting 102 amino acids, the leading ubiquitination site was also deleted, and OsCSN1 may have lost its ubiquitination function. Therefore, it could not respond to light signals and maintained its phenotype under normal light conditions, thereby affecting the expression of OsCSN1 in rice seed germination and the whole growth cycle. Therefore, it can be speculated that the region preceding the 102 amino acids at the N-terminus of CSN1 may have various functions, such as regulating the cell cycle, promoting cell division and proliferation, and being involved in the regulation of gene expression (Figure 1E).

3.2. The Effect of the N-Terminus of OsCSN1 on the Spatiotemporal Localization of OsCSN1, OsCSN1DN32, and OsCSN1DN102 under Red-Light Treatment

The GFP fusion protein was used to investigate the subcellular localization of OsCSN1 in different rice tissues, and the effect of the N-terminus on the expression of the GFP fusion protein was analyzed. During the confocal laser observation of the aboveground parts of the rice mutant plants, none of the stems of the plants expressed the GFP fusion protein. Regardless of whether the N-terminus was knocked out, GFP was always present in the coleoptiles. The expression levels of GFP in leaves varied.

Under normal light conditions (Figure S1A), the GFP fusion protein was expressed in the coleoptiles of the *OsCSN1DN102-GFP*-OE, *OsCSN1DN32-GFP*-OE, and *OsCSN1-GFP*-OE mutant plants. No fusion protein was expressed in the leaves of the *OsCSN1DN32-GFP*-OE or *OsCSN1-GFP*-OE mutant plants, whereas a high level of GFP was expressed in the leaves of the *OsCSN1DN102-GFP*-OE mutant plants. The roots of the *OsCSN1DN102-GFP*-OE and *OsCSN1DN32-GFP*-OE mutants did not express the GFP fusion protein, whereas the roots of the *OsCSN1-GFP*-OE mutant expressed low levels of the GFP fusion protein.

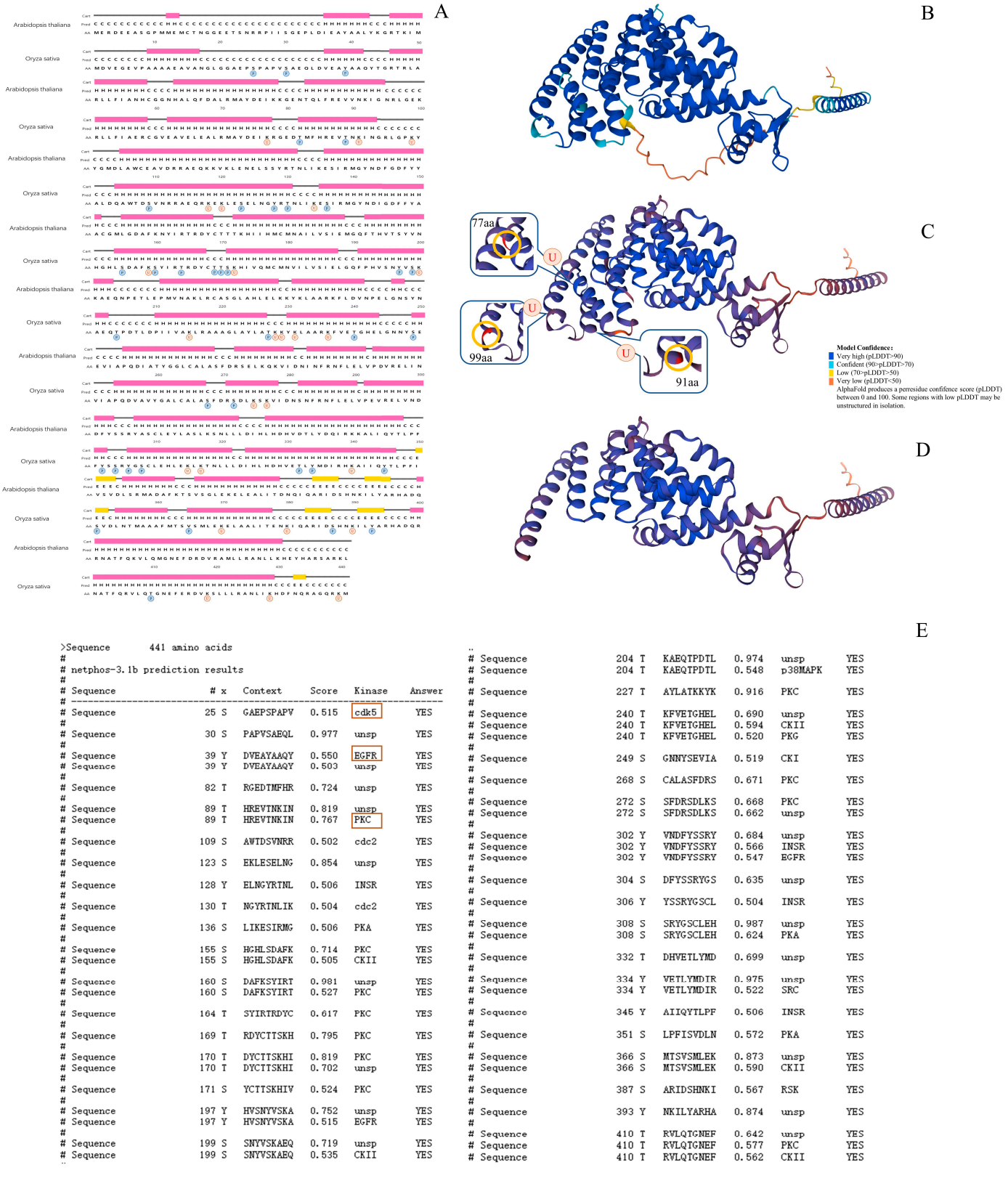


```
>Sequence       441 amino acids
#
# netphos-3.1b prediction results
#
# Sequence              # x   Context     Score   Kinase   Answer
# ------------------------------------------------------------------
# Sequence              25 S  GAEPSPAPV  0.515   cdk5     YES
#
# Sequence              30 S  PAPVSAEQL  0.977   unsp     YES
#
# Sequence              39 Y  DVEAYAAQY  0.550   EGFR     YES
# Sequence              39 Y  DVEAYAAQY  0.503   unsp     YES
#
# Sequence              82 T  RGEDTMFHR  0.724   unsp     YES
#
# Sequence              89 T  HREVTNKIN  0.819   unsp     YES
# Sequence              89 T  HREVTNKIN  0.767   PKC      YES
#
# Sequence             109 S  AWTDSVNRR  0.502   cdc2     YES
#
# Sequence             123 S  EKLESELNG  0.854   unsp     YES
#
# Sequence             128 Y  ELNGYRTNL  0.506   INSR     YES
#
# Sequence             130 T  NGYRTNLIK  0.504   cdc2     YES
#
# Sequence             136 S  LIKESIRMG  0.506   PKA      YES
#
# Sequence             155 S  HGHLSDAFK  0.714   PKC      YES
# Sequence             155 S  HGHLSDAFK  0.505   CKII     YES
#
# Sequence             160 S  DAFKSYIRT  0.981   unsp     YES
# Sequence             160 S  DAFKSYIRT  0.527   PKC      YES
#
# Sequence             164 T  SYIRTRDYC  0.617   PKC      YES
#
# Sequence             169 T  RDYCTTSKH  0.795   PKC      YES
#
# Sequence             170 T  DYCTTSKHI  0.819   PKC      YES
# Sequence             170 T  DYCTTSKHI  0.702   unsp     YES
#
# Sequence             171 S  YCTTSKHIV  0.524   PKC      YES
#
# Sequence             197 Y  HVSNYVSKA  0.752   unsp     YES
# Sequence             197 Y  HVSNYVSKA  0.515   EGFR     YES
#
# Sequence             199 S  SNYVSKAEQ  0.719   unsp     YES
# Sequence             199 S  SNYVSKAEQ  0.535   CKII     YES
..
# Sequence             204 T  KAEQTPDTL  0.974   unsp     YES
# Sequence             204 T  KAEQTPDTL  0.548   p38MAPK  YES
#
# Sequence             227 T  AYLATKKYK  0.916   PKC      YES
#
# Sequence             240 T  KFVETGHEL  0.690   unsp     YES
# Sequence             240 T  KFVETGHEL  0.594   CKII     YES
# Sequence             240 T  KFVETGHEL  0.520   PKG      YES
#
# Sequence             249 S  GNNYSEVIA  0.519   CKI      YES
#
# Sequence             268 S  CALASFDRS  0.671   PKC      YES
#
# Sequence             272 S  SFDRSDLKS  0.668   PKC      YES
# Sequence             272 S  SFDRSDLKS  0.662   unsp     YES
#
# Sequence             302 Y  VNDFYSSRY  0.684   unsp     YES
# Sequence             302 Y  VNDFYSSRY  0.566   INSR     YES
# Sequence             302 Y  VNDFYSSRY  0.547   EGFR     YES
#
# Sequence             304 S  DFYSSRYGS  0.635   unsp     YES
#
# Sequence             306 Y  YSSRYGSCL  0.504   INSR     YES
#
# Sequence             308 S  SRYGSCLEH  0.987   unsp     YES
# Sequence             308 S  SRYGSCLEH  0.624   PKA      YES
#
# Sequence             332 T  DHVETLYMD  0.699   unsp     YES
#
# Sequence             334 Y  VETLYMDIR  0.975   unsp     YES
# Sequence             334 Y  VETLYMDIR  0.522   SRC      YES
#
# Sequence             345 Y  AIIQYTLPF  0.506   INSR     YES
#
# Sequence             351 S  LPFISVDLN  0.572   PKA      YES
#
# Sequence             366 S  MTSVSMLEK  0.873   unsp     YES
# Sequence             366 S  MTSVSMLEK  0.590   CKII     YES
#
# Sequence             387 S  ARIDSHNKI  0.567   RSK      YES
#
# Sequence             393 Y  NKILYARHA  0.874   unsp     YES
#
# Sequence             410 T  RVLQTGNEF  0.642   unsp     YES
# Sequence             410 T  RVLQTGNEF  0.577   PKC      YES
# Sequence             410 T  RVLQTGNEF  0.562   CKII     YES
```

Figure 1. Structural analysis of OsCSN1. (**A**) Secondary structure comparison of OsCSN1 in rice and *Arabidopsis*, where P represents phosphorylation site and U represents ubiquitination site. (**B**) Prediction of OsCSN1 tertiary structure. (**C**) Prediction of OsCSN1DN32 tertiary structure. (**D**) Prediction of OsCSN1DN102 tertiary structure. (**E**) Prediction of OsCSN1 phosphorylation sites.

Under red-light treatment (Figure S1B), the coleoptiles of the *OsCSN1DN32-GFP*-OE, *OsCSN1DN102-GFP*-OE, and *OsCSN1-GFP*-OE mutants expressed the GFP fusion protein. The leaves of the *OsCSN1DN102-GFP*-OE mutant did not express the GFP fusion protein, whereas those of the *OsCSN1DN32-GFP*-OE mutant and *OsCSN1-GFP*-OE mutant expressed low levels of GFP fusion protein. A high amount of the GFP fusion protein was expressed in the roots of the *OsCSN1DN102-GFP*-OE mutant, whereas no GFP fusion protein was expressed in the roots of the *OsCSN1DN32-GFP*-OE or *OsCSN1-GFP*-OE mutants.

Under red light with a PAC treatment (Figure S1C), the coleoptiles of the *OsCSN1DN102-GFP*-OE, *OsCSN1DN32-GFP*-OE, and OsCSN1-GP-OE mutants expressed low levels of the GFP fusion protein. No GFP fusion protein was expressed in the leaves of the *OsCSN1DN102-GFP*-OE mutant, while the leaves of the *OsCSN1DN32-GFP*-OE mutant and *OsCSN1-GFP*-OE mutant expressed low levels of the GFP fusion protein. The roots of the OE mutants did not express GFP fusion proteins, while the roots of the *OsCSN1-GFP*-OE mutants expressed high level of the GFP fusion protein.

Under the red light with GA_3 treatment (Figure S1D), the GFP fusion protein was expressed in the leaves and coleoptiles of all mutants. A high amount of the GFP fusion protein was expressed in the coleoptiles of the *OsCSN1DN32-GFP*-OE mutant, whereas the *OsCSN1DN32-GFP*-OE and *OsCSN1DN102-GFP*-OE mutant plants did not express the GFP fusion protein in the roots, whereas the *OsCSN1-GFP*-OE mutant plants expressed more GFP fusion protein in the roots. Therefore, the localization of *OsCSN1-GFP* was not observed in rice stems, and the localization and expression of GFP fusion proteins in coleoptiles were not affected by light or hormones, nor were they affected by changes in the N-terminus. These results suggest that the localization of OsCSN1 in coleoptiles is relatively stable. For leaves, a large amount of the GFP fusion protein was expressed under normal light irradiation when OsCSN1N102 was knocked out. Under red-light treatment, the expression of the GFP fusion protein was eliminated when the N102 region of OsCSN1 was knocked out. These results show that red light changed the localization of OsCSN1 in leaves and promoted the localization of OsCSN1 in leaves. Red light and the hormone GA promoted the localization of OsCSN1 in leaves but were not affected by the GA inhibitor PAC. Red light affected the localization of OsCSN1 in leaves. In the root system, OsCSN1 was not located in the roots under normal light irradiation, but under red light, the N102 knockout of OsCSN1 promoted the expression of the GFP fusion protein. CSN1 promoted the expression of GFP fusion proteins in roots when GA3 and PAC were added, whereas the N-terminal deletion of CSN1 did not result in the expression of GFP fusion proteins.

3.3. OsCSN1 Is a Negative Regulator of Rice Seedling Stem Elongation Regulated by Red Light

Under light treatment, the heights of the *oscsn1-1* mutant, *oscsn1-2* mutant, OsCSN1-OE mutant, *OsCSN1DN32-GFP*-OE mutant, and *OsCSN1DN102-GFP*-OE mutant plants were greater than those of the WT plants; the *oscsn1-2* mutant had the most significant height, while the *OsCSN1-GFP*-OE mutant had the shortest height (Figure 2A,B). These results indicated that CSN1 may be a negative regulator of rice-seedling growth.

Compared with those in the light treatment, the heights of the WT plants and *OsCSN1-GFP*-OE mutants in the red-light treatment were significantly greater, and the heights of *oscsn1-1*, *oscsn1-2*, and *OsCSN1DN102-GFP*-OE mutants were significantly lower. (Figure 2D,E). The results showed that the *OsCSN1-GFP*-OE mutant was sensitive to red light, whereas *oscsn1-1*, *oscsn1-2*, *OsCSN1DN102-GFP*-OE, and *OsCSN1DN32-GFP*-OE mutants were insensitive to red light. The negative effects caused by monochromatic red light can reduce plant biomass and leaf area and cause excessive stem elongation [24]. *oscsn1-1*, *oscsn1-2*, *OsCSN1DN32-GFP*-OE, and *OsCSN1DN102-GFP*-OE plants were insensitive to red light. It has been speculated that red light may affect shoot elongation in rice plants by regulating OsCSN1, and the functional domain may be at the N-terminus.

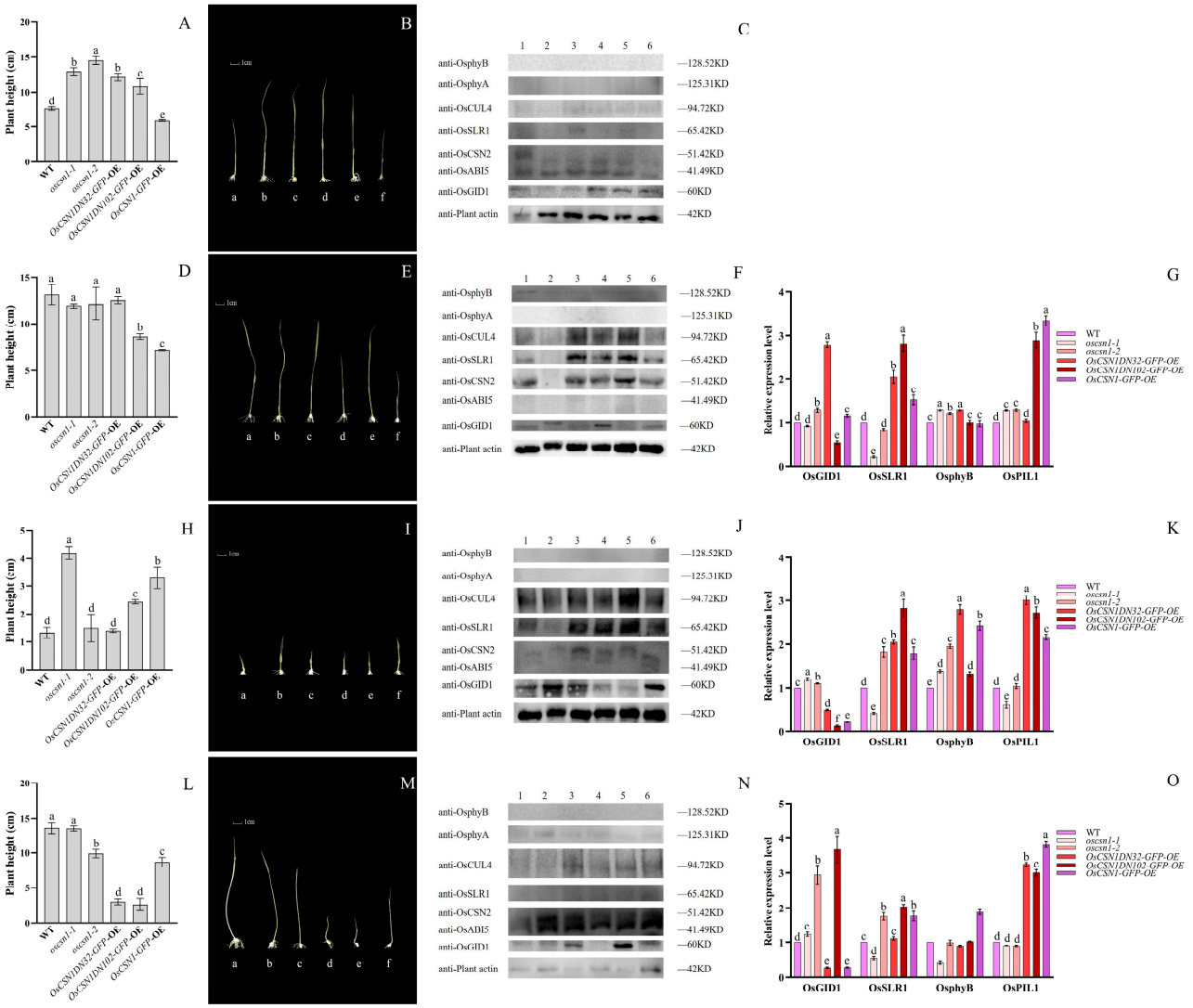

Figure 2. Analysis of plant under red-light and hormone conditions. (**A**) Plant height data graph of WT and *OsCSN1* mutants grown under light. (N = 5; Statistical significance was set at $p \leq 0.05$). (**B**) Plant height phenotype of WT and *OsCSN1* mutants grown under light. (**C**) Protein expression of wild type and *OsCSN1* mutants grown 9d under light. Detection of OsphyA, OsphyB, OsABI5, OsSLR1, OsCSN2, OsGID1, and OsCUL4 levels in sample lines by Western blot. (**D**) Plant height data graph of WT and *OsCSN1* mutants grown under red light. (N = 5; Statistical significance was set at $p \leq 0.05$). (**E**) Plant height phenotype of WT and *OsCSN2* mutants grown under red light. (**F**) Protein expression of wild type and *OsCSN1* mutants grown 9 d under red light. Detection of OsphyA, OsphyB, OsABI5, OsSLR1, OsCSN2, OsGID1, and OsCUL4 levels in sample lines by Western blot. (**G**) Expression of genes associated with WT and *OsCSN1* mutants grown for 9 d under red-light treatment at the mRNA level. (**H**) Plant height data graph of WT and *OsCSN1* mutants grown under red light and PAC. (N = 5; Statistical significance was set at $p \leq 0.05$). (**I**) Plant height phenotype of WT and *OsCSN2* mutants grown under red light and PAC. (**J**) Protein expression of wild type and *OsCSN1* mutants grown 9d under red light and PAC. Detection of OsphyA, OsphyB, OsABI5, OsSLR1, OsCSN2, OsGID1, and OsCUL4 levels in sample lines by Western blot. (**K**) Expression of genes associated with WT and *OsCSN1* mutants grown for 9 d under red light and PAC of treatment at the mRNA level. (**L**) Plant height data graph of WT and *OsCSN1* mutants grown under red light and GA. (N = 5; Statistical significance was set at $p \leq 0.05$). (**M**) Plant height phenotype of WT and *OsCSN2* mutants grown under red light and GA. (**N**) Protein expression of wild type and *OsCSN1* mutants grown 9 d under red light and GA. Detection of OsphyA, OsphyB, OsABI5, OsSLR1, OsCSN2,

OsGID1, and OsCUL4 levels in sample lines by Western blot. (**O**) Expression of genes associated with WT and *OsCSN1* mutants grown for 9 d under red light and GA of treatment at the mRNA level. (1: WT; 2: *oscsn1-1*; 3: *oscsn1-2*; 4: *OsCSN1DN32-GFP*-OE; 5: *OsCSN1DN102-GFP*-OE; 6: *OsCSN1-GFP*-OE) (a: WT; b: *oscsn1-1*; c: *oscsn1-2*; d: *OsCSN1DN32-GFP*-OE; e: *OsCSN1DN102-GFP*-OE; f: *OsCSN1-GFP*-OE).

PAC can inhibit the expression of the endogenous plant hormone GA3, delay plant growth, and inhibit stem elongation. Under PAC with red-light treatment, the growth of all plants was significantly inhibited, and the heights of the *oscsn1-1* and *OsCSN1DN102-GFP*-OE mutant plants were significantly inhibited, indicating that under red-light treatment, the *oscsn1-1* and *OsCSN1DN102-GFP*-OE plants exhibited attenuated sensitivity to PAC (Figure 2H,I). After adding PAC, the adverse effects caused by red light were reduced. Therefore, red light may affect plant growth and development through the CSN1-mediated endogenous GA-signaling pathway.

After treatment with the exogenous hormone GA3 with red light, the plant height of the WT was not affected, whereas the plant heights of the *oscsn1-1* mutant, *OsCSN1DN32-GFP*-OE mutant, and *OsCSN1DN102-GFP*-OE mutant were inhibited, indicating that excessive exogenous GA inhibited the plant-growth phenotype (Figure 2L,M). The height of *OsCSN1-GFP*-OE mutant plants was significantly greater after adding GA3, and *OsCSN1-GFP*-OE plants were sensitive to red light. Thus, in response to red light, OsCSN1 acts as a negative regulator of stem elongation in rice plants. Red light may regulate the GA-signaling pathway through OsCSN1, thereby affecting the growth and development of rice plants. The OsCSN1 domain may be located at the N terminus of OsCSN1.

3.4. OsCSN1 Is a Positive Regulator of Red-Light-Regulated Coleoptile Elongation in Seedlings

A typical feature of rice photomorphogenesis is the inhibition of coleoptile elongation under light treatment. Under light treatment, the coleoptiles of the *OsCSN1DN102-GFP*-OE and *OsCSN1-GFP*-OE mutants were longer than those of the WT, and the coleoptiles of the *oscsn1-1*, *oscsn1-2*, and *OsCSN1DN102-GFP*-OE mutants were shorter than those of the WT. Under light treatment, the expression of the GFP fusion protein was detected in the coleoptiles of the three mutants. The expression level in the *OsCSN1DN32-GFP*-OE mutant was greater than that in the *OsCSN1DN102-GFP*-OE mutant and *OsCSN1-GFP*-OE mutant, and the proteins were distributed mainly near the coleoptile veins. *OsCSN1DN32-GFP*-OE mutants expressed the most GFP fusion protein and the shortest coleoptile. Although *OsCSN1DN102-GFP*-OE and *OsCSN1-GFP*-OE plants expressed the GFP fusion protein, the coleoptiles were relatively long (Figures 3A,B and S2A). These results indicate that OsCSN1 is involved in coleoptile elongation and photomorphogenesis in rice. This result is consistent with previous studies in Arabidopsis, showing that CSN1 is critical for the structural integrity of the CSN and that AtCSN is a negative regulator of photomorphogenesis.

A previous study showed that red light could inhibit plant coleoptile elongation [34]. However, under red-light treatment, the number of coleoptiles of the *OsCSN1DN102-GFP*-OE mutant, *OsCSN1DN32-GFP*-OE mutant, *oscsn1-1* mutant, and *oscsn1-2* mutant increased significantly compared to that under light treatment, indicating an inhibitory effect of red light on the coleoptiles of rice plants. However, this effect was not significant. The expression of the *OsCSN1-GFP* fusion protein was detected in the coleoptile of the *OsCSN1-GFP*-OE mutant, and the elongation of the coleoptile was significantly inhibited, indicating that the *OsCSN1-GFP*-OE mutant is sensitive to red light (Figures 3C,D and S2B). These results indicate that the inhibitory effect of red light on rice coleoptile elongation requires the participation of intact OsCSN1.

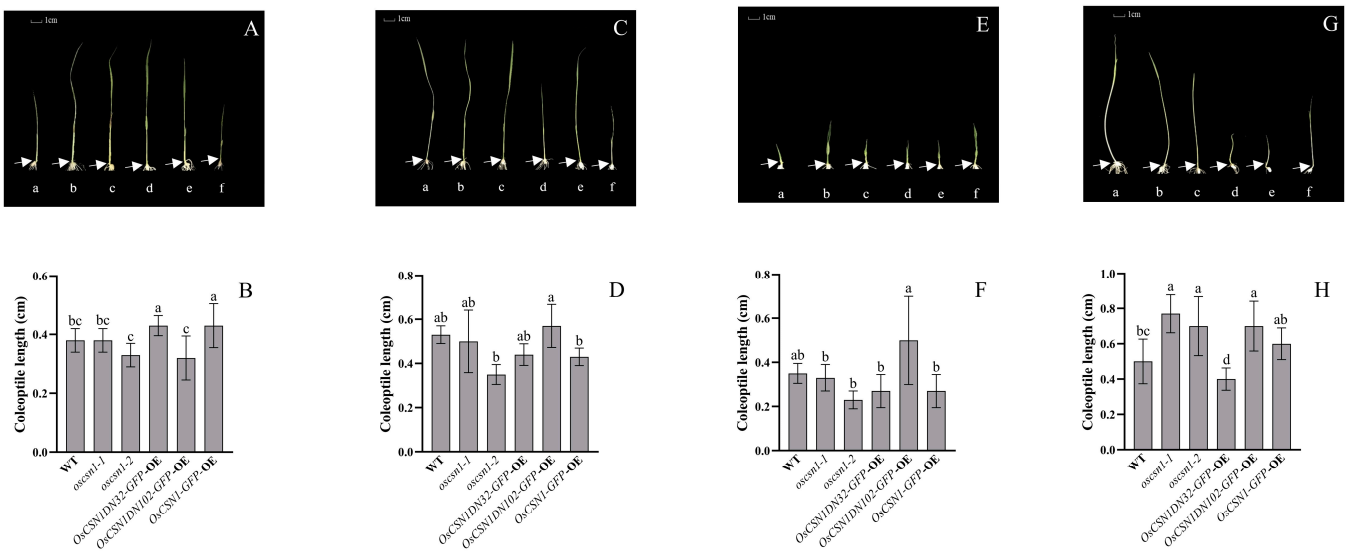

Figure 3. Analysis of coleoptile under red-light and hormone conditions. (**A**) Coleoptile phenotype of WT and *OsCSN1* mutants grown under light. (**B**) Coleoptile length data graph of WT and *OsCSN1* mutants grown under light. (N = 5; Statistical significance was set at $p \leq 0.05$). (**C**) Coleoptile phenotype of WT and *OsCSN1* mutants grown under red light. (**D**) Coleoptile length data graph of WT and *OsCSN1* mutants grown under red light. (N = 5; Statistical significance was set at $p \leq 0.05$). (**E**) Coleoptile phenotype of WT and *OsCSN1* mutants grown under red light and PAC. (**F**) Coleoptile length data graph of WT and *OsCSN1* mutants grown under red light and PAC. (N = 5; Statistical significance was set at $p \leq 0.05$). (**G**) Coleoptile phenotype of WT and *OsCSN1* mutants grown under red light and GA. (**H**) Coleoptile length data graph of WT and *OsCSN1* mutants grown under red light and GA. (N = 5; Statistical significance was set at $p \leq 0.05$). (a: WT; b: *oscsn1-1*; c: *oscsn1-2*; d: *OsCSN1DN32-GFP*-OE; e: *OsCSN1DN102-GFP*-OE; f: *OsCSN1-GFP*-OE).

Red light has an inhibitory effect on rice coleoptiles by inhibiting excessive elongation. Under PAC with red-light treatment, the coleoptile length of the *OsCSN1-GFP*-OE mutant was significantly shorter than that under light treatment, indicating that this mutant was sensitive to PAC. The coleoptile lengths of the other mutants were similar to those of the plants subjected to light treatment, and these mutants were sensitive to PAC. In sensitive cells, the elongation of the coleoptile was not inhibited by PAC. Under red-light treatment, the addition of GA3 rescued the inhibitory effect of red light on the *oscsn1-1*, *oscsn1-2*, *OsCSN1DN102-GFP*-OE, and *OsCSN1-GFP*-OE mutants (Figures 3E,F and S2C). Under GA3 with the red-light treatment, the coleoptiles of the *oscsn1-1* mutant, *oscsn1-2* mutant, and *OsCSN1DN102-GFP*-OE mutant were significantly elongated, whereas those of the *OsCSN1-GFP*-OE mutant and the *OsCSN1DN32-GFP*-OE mutant were elongated, but the difference was not significant. After the addition of GA3, the sensitivity of the coleoptile of the *OsCSN1DN32-GFP*-OE mutant to red light increased, the sensitivity of the coleoptile of the *OsCSN1DN102-GFP*-OE mutant to red light was unchanged, and the coleoptiles of the *OsCSN1-GFP*-OE mutant were sensitive to red light. The light sensitivity was reduced (Figures 3G,H and S2D). Exogenous GA could rescue the effect of red light on the inhibition of coleoptile elongation in the *OsCSN1DN32-GFP*-OE and *OsCSN1-GFP*-OE mutants. Therefore, OsCSN1 plays an essential regulatory role in the red-light-mediated inhibition of rice coleoptile elongation. It regulates the GA-signaling pathway to affect the growth and development of rice coleoptiles, and the regulatory domain may be located at the N-terminus of CSN1.

3.5. Regulatory Effect of OsCSN1 on the Tap Root Extension of Rice Plants under Red Light

Under light conditions, the growth of the tap roots of the *OsCSN1DN102-GFP*-OE mutant did not change significantly, whereas that of the other mutants increased significantly,

with the most significant difference between the *oscsn1-1* mutant and WT plants occurring in the absence of GFP fusion protein expression (Figures 4A,B and S3A). Red light inhibited the extension of rice tap roots (Figure 4C,F). Under red-light treatment, the roots of the *oscsn1-1* and *oscsn1-2* mutant plants grew significantly, and the roots of the *OsCSN1DN102-GFP*-OE and *OsCSN1-GFP*-OE mutant plants were significantly shorter. Furthermore, there was no expression of the GFP fusion protein in the roots of the *OsCSN1DN32-GFP*-OE mutant or *OsCSN1-GFP*-OE mutant plants. The expression level of the GFP fusion protein in the *OsCSN1DN102-GFP*-OE mutant was higher (Figure S3B). Extensions in the tap roots of the *oscsn1-1*, *oscsn1-2*, *OsCSN1DN102-GFP*-OE, and *OsCSN1DN32-GFP*-OE mutants were insensitive to red-light inhibition. In contrast, the *OsCSN1-GFP*-OE mutant was sensitive to red-light inhibition.

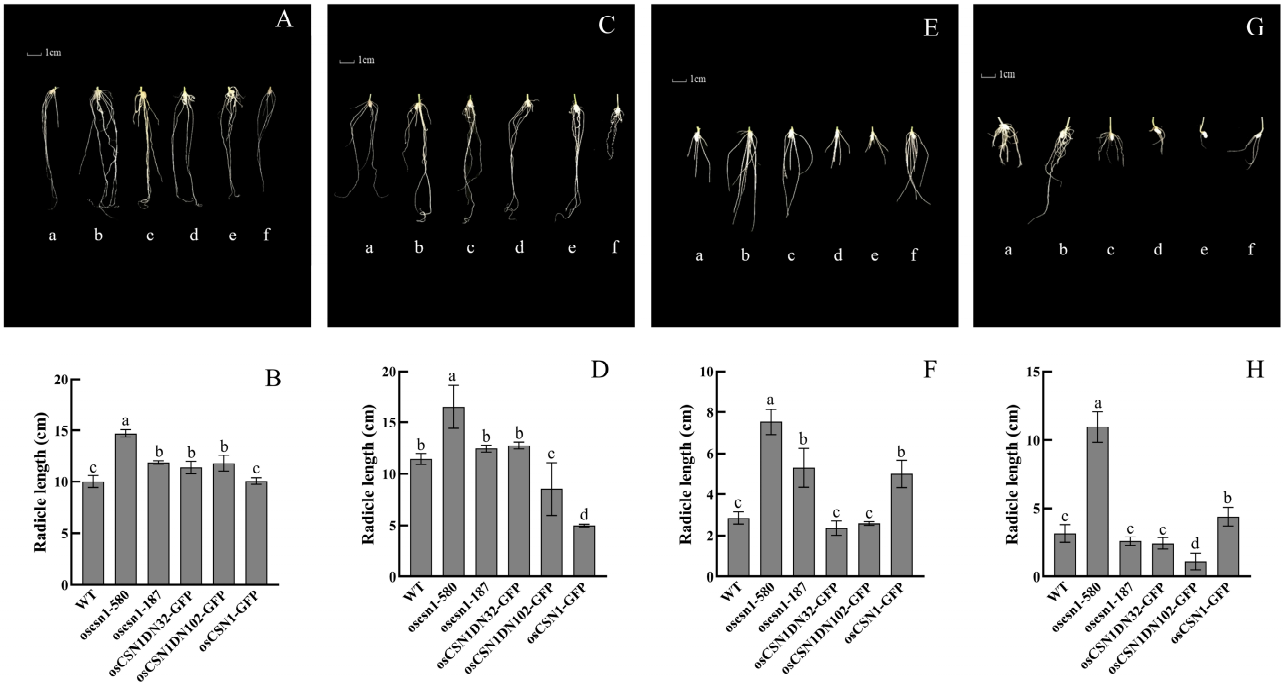

Figure 4. Analysis of root under red-light and hormone conditions. (**A**) Root phenotype of WT and *OsCSN1* mutants grown under light. (**B**) Root-length data graph of WT and *OsCSN1* mutants grown under light. (N = 5; Statistical significance was set at $p \leq 0.05$). (**C**) Root phenotype of WT and *OsCSN1* mutants grown under red light. (**D**) Root-length data graph of WT and *OsCSN1* mutants grown under red light. (N = 5; Statistical significance was set at $p \leq 0.05$). (**E**) Root phenotype of WT and *OsCSN1* mutants grown under red light and PAC. (**F**) Root-length data graph of WT and *OsCSN1* mutants grown under red light and PAC. (N = 5; Statistical significance was set at $p \leq 0.05$). (**G**) Root phenotype of WT and *OsCSN1* mutants grown under red light and GA. (**H**) Root-length data graph of WT and *OsCSN1* mutants grown under red light and GA. (N = 5; Statistical significance was set at $p \leq 0.05$). (a: WT; b: *oscsn1-1*; c: *oscsn1-2*; d: *OsCSN1DN32-GFP*-OE; e: *OsCSN1DN102-GFP*-OE; f: *OsCSN1-GFP*-OE).

Red light inhibits the elongation of tap roots in rice plants. In the aboveground plant parts, both low and high concentrations of PAC inhibited the elongation of coleoptiles and stems. However, low concentrations of PAC (less than 10^{-6} mol/L) could promote tap root extension in dark-grown rice plants, and high concentrations of PAC (greater than 10^{-5} mol/L) could inhibit tap root extension [50]. Under the PAC with red-light treatment, except for the *OsCSN1-GFP*-OE mutant, the root length of all samples was significantly shorter than that under red-light treatment, and the *OsCSN1DN32-GFP*-OE mutant and *OsCSN1DN102-GFP*-OE mutant did not express the GFP fusion protein. *OsCSN1-GFP*-OE mutants expressed a high level of GFP fusion protein. This difference may be due to the inhibitory effect of red light on root length. Another reason might be that a high

concentration of PAC (greater than 10^{-5} mol/L) could inhibit the extension of tap roots. In contrast, the root length of the *OsCSN1-GFP*-OE mutant did not change under red light or PAC with red-light treatment, indicating that the *OsCSN1-GFP*-OE mutant was not sensitive to exogenous PAC under red-light treatment (Figures 4E,F and S3C).

Under the GA3 with red-light treatment, the length of the tap roots of all the rice species decreased, indicating that the addition of exogenous GA did not promote the extension of the tap roots of the rice plants; moreover, these findings indicate that the signaling pathway involved in the elongation of the tap roots of the rice plants was not significantly related to the GA-signaling pathway (Figures 4G,H and S3D).

3.6. The Effect of OsCSN1 Signal Transduction on the Growth and Development of Rice Plants at the Seedling Stage

To further analyze the signaling pathway of OsCSN1 in the process of red-light-regulated growth and development in rice plants, we detected changes in the gene expression levels of OsGID1, OsSLR1, OsphyB, and OsPIL1 in the above-depicted rice mutant seedlings under different treatments. Further, we investigated the involvement of OsCSN1 in metabolic regulation. Furthermore, at the protein level, changes in the expression levels of OsphyB, OsABI5, OsSLR1, OsCUL4, and OsCSN2 were detected to analyze and validate the signaling role of OsCSN1 in rice-seedling growth and development.

Under light treatment, the expression levels of OsSLR1 in the *oscsn1-1* and *OsCSN1DN32-GFP*-OE mutants were very low and could hardly be detected. The expression levels of OsSLR1 in the *oscsn1-2* mutant and *OsCSN1DN102-GFP*-OE mutant were lower than that in the WT, whereas the *OsCSN1-GFP*-OE mutant had the highest expression level of OsSLR1. Under light treatment, the *OsCSN1-GFP*-OE mutant had the highest expression level of OsABI5, whereas the *oscsn1-1* mutant, *oscsn1-2* mutant, and *OsCSN1DN32-GFP*-OE mutant had lower OsABI5 expression levels than the WT (Figure 2C). The expression level of OsABI5 in the *OsCSN1DN102-GFP*-OE mutant was similar to that in the WT because of the photolysis characteristics of OsphyB, and the expression of OsphyB was not detected in any of the rice plants, as mentioned above.

OsSLR1 is a negative regulator of the rice GA-signaling pathway. The results of the fluorescence quantitative detection showed that under red-light treatment, the expression level of OsSLR1 in the *OsCSN1DN102-GFP*-OE mutant was significantly upregulated. The expression levels of *OsCSN1DN32-GFP*-OE and *OsCSN1-GFP*-OE were also upregulated compared to those in the WT. In contrast, the expression level of OsSLR1 was significantly downregulated in the 1 mutant and *oscsn1-2* mutant (Figure 2G). The results of fluorescence-based quantitative analysis of OsGID1, another receptor protein in the GA-signaling pathway, revealed that under red-light treatment, the expression level of the OsGID1 gene in the *OsCSN1DN32-GFP*-OE mutant was significantly upregulated. The expression level of the OsGID1 gene in the *oscsn1-2* mutant and *OsCSN1-GFP*-OE mutant was significantly upregulated. The expression level of the OsGID1 gene also tended to increase, while the expression level of the OsGID1 gene in the *oscsn1-2* mutant and *OsCSN1DN102-GFP*-OE mutant decreased. A study of OsphyB gene expression showed that the expression levels of the *oscsn1-1* mutant, *oscsn1-2* mutant, and *OsCSN1-DN32GFP*-OE mutant were upregulated, whereas the remaining mutants exhibited little difference. Based on the above quantitative fluorescence results, we speculated that OsCSN1 might regulate the growth and development of rice plants by regulating the degradation of OsSLR1. We performed analysis and validation at the protein level to validate this inference further.

Under the red-light treatment (Figure 2F), the expression levels of OsSLR1 and OsABI5 in the *oscsn1-1* mutant were very low. The *OsCSN1DN102-GFP*-OE mutant exhibited the highest expression levels of OsSLR1 and OsABI5. The *oscsn1-2* and *OsCSN1DN32-GFP*-OE plants expressed a high level of OsSLR1, whereas the expression level of OsABI5 was very low. OsCSLR1 expression was higher in *OsCSN1-GFP*-OE plants than in WT plants, whereas OsABI5 expression levels were similar to those in WT plants. Therefore, the deletion of OsCSN1 affected the expression of OsSLR1, whereas the expression level of

OsABI5 did not change significantly. Therefore, under red-light treatment, OsCSN1 can affect the expression of OsSLR1 through the GA pathway to regulate plant growth, whereas the ABA-signaling pathway does not play a leading role in this process.

Under the red-light treatment, significant differences in rice OsphyB expression were also observed. OsphyB was the most highly expressed gene in the *oscsn1-1* mutant, followed by the *OsCSN1DN32-GFP*-OE mutant, which also had higher OsphyB expression levels, and the *OsCSN1-GFP*-OE mutant, which had the lowest expression level. phyB is a positive regulator that affects plants by controlling their height. The OsphyB expression level was consistent with the results, showing that the plant height of the *oscsn1-1* mutant was shorter than that of the light-treatment group. The plant height of the *OsCSN1-GFP*-OE mutant was greater than that of the light-treatment group. The *oscsn1-1* and *OsCSN1DN32-GFP*-OE mutants expressed the most OsphyB, but neither the extension of the tap roots nor the elongation of the stems were affected by red light. *OsCSN1-GFP*-OE plants expressed lower levels of OsphyB but exhibited an insensitive phenotype to the influence of red light. The *oscsn1-2* mutant and *OsCSN1DN32-GFP*-OE mutant had moderate OsphyB expression levels, and their phenotype showed weak sensitivity to red light. Therefore, it was speculated that OsphyB senses red light and regulates rice-seedling growth and development through OsCSN1.

After treatment with red light with PAC (Figure 2K), the results of the fluorescence quantification showed that the OsSLR1 expression levels in the *OsCSN1DN102-GFP*-OE mutant and *OsCSN1DN32-GFP*-OE mutant were significantly upregulated. In contrast, those in the *OsCSN1-GFP*-OE and *OsCSN1DN32-GFP*-OE mutant were significantly upregulated. The upregulation trend of the *oscsn1-2* mutant was similar, whereas that of the *oscsn1-1* mutant showed a trend toward downregulation. Moreover, OsGID1 in the *oscsn1-1* and *oscsn1-2* mutants tended to be downregulated, and the OsGID1 gene tended to be downregulated in the other overexpression mutants, regardless of whether the N-terminus of OsCSN1 was deleted. After the addition of PAC, the *oscsn1-1* mutant had the lowest expression levels of OsSLR1 and OsABI5, and the expression levels of the remaining mutants were greater than those of the WT. Similarly, the expression levels of OsSLR1 and OsABI5 in the *oscsn1-2* and *OsCSN1DN32-GFP*-OE mutants were more significant than those in the WT (Figure 2J).

Similarly, in the *OsCSN1DN102-GFP*-OE mutant, the expression level of OsSLR1 was lower, whereas the expression level of OsABI5 was higher. *OsCSN1-GFP*-OE mutants had higher expression levels of OsSLR1 and lower expression levels of OsABI5. Almost no phyB expression was detected after the addition of PAC, indicating that under these conditions, the inhibitory effect of PAC was far more significant than that of red light. The results of the fluorescence quantification showed that the expression levels of OsphyB were upregulated in all mutants, of which *OsCSN1DN32-GFP*-OE had the most significant upregulation. After the addition of PAC, the plant height of the mutants decreased. After the addition of GA, the height of the *OsCSN1-GFP*-OE mutant plants was strongly sensitive to red light, whereas that of the *oscsn1-1* mutant, *oscsn1-2* mutant, and *OsCSN1DN32-GFP*-OE mutant plants were insensitive to red light, indicating that exogenous GA can promote the expression of OsphyB, exogenous PAC can inhibit the expression of OsphyB, and the deletion of OsCSN1 or N-terminal deletion can affect the expression of OsphyB. The results showed that under red light with PAC treatments, the effect of PAC was more significant than that under red light, and the *oscsn1-1* mutant had the weakest sensitivity to the inhibition of PAC. OsphyB senses red light and regulates the GA-signaling pathway to affect the growth and development of rice plants through CSN1. The main regulatory domain is located at the N-terminus of CSN1. The N-terminal domain of CSN is related mainly to the photoreception and light-signal transduction of phytochrome. In contrast, the C-terminal domain is involved mainly in the formation of phytochrome dimers and interactions with downstream signaling molecules [51]. The results of our study are consistent with these findings.

After treatment with red light with GA (Figure 2O), the results of the fluorescence quantification showed that OsSLR1 and OsGID1 were significantly upregulated in the *OsCSN1DN102-GFP*-OE mutant and *oscsn1-2* mutant, and the *OsCSN1DN32-GFP*-OE mutant, *OsCSN1-GFP*OE mutant, and *OsCSN1-GFP*-OE mutant were significantly upregulated. The expression level of OsSLR1 in the mutant was upregulated but not significantly. The expression level of OsSLR1 in the *oscsn1-1* mutant was downregulated, but the upregulation trend of OsGID1 was minimal. The expression level of OsGID1 in the *OsCSN1DN32-GFP*-OE and *OsCSN1-GFP*-OE mutants did not change. After treatment with red light with GA (Figure 2N), all mutants expressed more OsSLR1 than the WT plants, especially *oscsn1-1* and *oscsn1-2*, and the expression level of OsSLR1 was the lowest in the *OsCSN1-GFP*-OE mutant. However, the expression level of OsABI5 in the *oscsn1-1* mutant was lower than that in the WT, the expression level of OsABI5 in the *OsCSN1-GFP*-OE mutant was similar to that in the WT, and the expression levels of the other mutants were more significant than those in the WT. After adding GA, the expression level of phyB increased in all the plants, and the expression level of OsphyB in the *oscsn1-1* and *oscsn1-2* mutants was the highest. The expression level in the *OsCSN1-GFP*-OE mutant was the lowest, and the expression level in the *OsCSN1DN32-GFP*-OE mutant was the lowest. In both mutant and *OsCSN1DN102-GFP*-OE plants, the expression level of OsphyB in the mutant was similar to that in the WT. These results indicated that only the expression level of the *OsCSN1-GFP*-OE mutant OsphyB was upregulated.

With the addition of GA, the sensitivity of the *oscsn1-1* and *oscsn1-2* mutants to red light was still very weak, and external GA did not enhance the negative effect of red light on plants. Under red light with the GA treatment, the expression levels of OsSLR1 and ABI5 in the *OsCSN1-GFP*-OE mutant decreased, and the negative effect of red light on plants increased in response to the addition of GA. OsCSN1 can regulate the response of rice plants to red light at the seedling stage by regulating the degradation of OsSLR1, thereby affecting plant growth and development. The effect of red light on the plant's aboveground parts was more significant. The domains involved in this regulation may be related to the N terminus of OsCSN1.

4. Discussion

4.1. The Structure of OsCSN1 Is Conserved, and the Ubiquitination Site at the N-Terminus Regulates the Function and Spatiotemporal Positioning of CSN

Ubiquitination is a post-translational modification of proteins at lysine residues and plays a crucial role in regulating the balance of proteins and enzymes in plants. It accounts for approximately 6% of genes in Arabidopsis. It encodes the ubiquitin-26s proteasome component. This protein-degradation pathway involves plant morphogenesis, flowering, photoperiod, and hormone regulation. CSN can regulate the plant's response to light signals through the ubiquitin-degradation pathway, thus enabling plants to complete the transition from dark growth to light morphogenesis. The currently known modification substrates of NEDD8/RUB1 are limited to the CULLIN protein and p53, with the former being SCF or a subunit of E3, similar to SCF. The RUB1 modification of CULLIN and CULLIN4 can activate the E3 ligases to which they belong. Experiments in Arabidopsis have shown that the CUL4 E3 complex can form a complex with CDD. In contrast, CSN can modify CUL4 to remove RUB1 to inhibit its activity, thus causing phenotypic changes in plant photomorphogenesis.

Although the Arabidopsis mutant fus6/C231 lacking the CSN1-N end can form a CSN complex structure, and the deneddylation activity of CSN is unaffected, this mutant exhibits a closed cotyledon phenotype. This indicates that the AtCSN1 N-terminal domain is required for light-dependent cotyledon opening. More importantly, the AtCSN1 N-terminus was required to produce true leaves through the shoot apex, indicating the transition from seedling to normal plant development. It is possible that the ubiquitination locus associated with the regulatory functions of some genes was missing. This indicates that the N-terminus of CSN1 has special functions in plant development and is related

to the essential physiological functions of CSN1. The N-terminus of CSN1 regulates the de-ubiquitination of the CSN complex, affects the degradation of proteins by the ubiquitin–proteasome system, regulates the stability of related proteins in the complex hormone network in rice, and ultimately regulates the growth and development of rice.

Protein structure analysis revealed that the α-helix at the N-terminus of OsCSN1 contained six more amino acids than that of AtCSN1; the end of OsCSN1 at the C-terminus was a β-sheet and random coil, but AtCSN1 was not. These structural changes might endow OsCSN1 with different functions.

Our results showed that the coleoptile sheaths, stem elongation, coleoptile elongation, and tap root elongation of the OsCSN1 mutant with the deletion of the 102 amino acid at the N-terminus were insensitive to red light, and the mutants produced and developed typically and set fruit, which is consistent with the findings of previous studies on *Arabidopsis thaliana*. Arabidopsis plants lacking the CSN1-N-terminus can form the CSN complex structure under normal growth conditions, and the deneddylation activity of CSN is not affected; however, these plants exhibit a dark phenotype. This finding indicates that the N-terminal domain of OsCSN1, similar to the N-terminal domain of AtCSN1, is required for light-dependent growth.

Under all treatments, the fusion proteins were expressed in the coleoptiles with the N-terminal deletion of 32 amino acids and the deletion of 102 amino acid mutants. Under red light with PAC treatment, a low amount of the GFP fusion protein was expressed in the coleoptiles of the OsCSN1-overexpressing plants. In addition, the length of the coleoptile and the expression levels of OsSLR1, OsGID1, OsPIL14, and OsphyB in the DN32 mutants were similar to those in the OsCSN1 overexpression mutants, indicating that 32 at the N-terminus of OsCSN1 is involved in the process of the red-light inhibition of rice coleoptile elongation. Under all treatments, the changes in coleoptile length and expression levels of OsSLR1, OsGID1, PIL14, and phyB in the DN102 mutants were the same as those in the OsCSN1-deletion mutants. The results showed that 32-102 amino acid at the N-terminus of OsCSN1 was the main domain that inhibited rice coleoptile elongation through red light. OsCSN1 is involved in the regulatory effect of red light on the elongation of rice coleoptiles, mainly through the ubiquitination of three key ubiquitination sites at positions 77, 91, and 99, affecting the degradation of SLR1 and PIFs and inhibiting the elongation of coleoptiles.

Moreover, our study showed that OsCSN1 mutants with 102 amino acid deletions at the N-terminus were more insensitive to red light than OsCSN1 mutants with 32 amino acid deletions at the N-terminus. The three key ubiquitination sites at position 99 reduce the sensitivity of the mutants to red light. However, further studies are needed to determine which phosphorylation or ubiquitination site at positions 77, 91, or 99 endows the N-terminus with special functions.

4.2. Under Red-light treatment, OsCSN1, an Essential Component of the CSN, Degrades SLR1 through De-Neddylation, Promotes the Expression of PIL11, and Promotes the Elongation of Rice Stems

Compared to white light, red light can reduce plant biomass and leaf area, cause excessive stem elongation, and affect leaf number and chlorophyll content. In Arabidopsis, the PIF3 protein was the first to interact with phytochromes. It has been reported that the interactions between the C-terminal ends of phyB and phyA and between the C-terminal ends of the PIF3 protein were verified through yeast two-hybrid experiments [52]. Using biological methods such as genetics and reverse genetics, phytochrome-interacting proteins, such as PIF4, PIF5, and PIF6 [53–55], which are the currently known members of the PIF family in Arabidopsis, have been identified. Eight proteins (PIF1, PIF3-PIF8, and PIL1, later named PIF2) have slightly different molecular characteristics and functions [48,56]. Through homologous sequence analysis, six phytochrome-interaction factors were predicted in the rice genome and named OsPIL11-OsPIL16. OsPIL13 and OsPIL14 in rice are highly homologous to Arabidopsis PIF4 and PIF5, and OsPIL15 and OsPIL16 are related to PIF3. This sequence has a high homology.

The heights of the OsCSN1-deletion mutants and reduced mutant plants were insensitive to red light. The expression levels of OsSLR1 and OsABI5 in the deletion mutants were very low, but the expression level of OsSLR1 in the reduced mutants was high, indicating that deletion or reduction of OsCSN1 affects OsSLR1. Moreover, both mutants increased the expression levels of phyB, GID1, CSN2, PIL11, and CUL1. It is speculated that OsCSN1 regulates neddylation through CSN to degrade the negative regulator SLR1 in the GA pathway, thereby inhibiting the degradation of PIL11 and, eventually, the inhibition of stem elongation. Furthermore, the heights of the OsCSN1-deletion mutants and reduced mutant plants under red-light treatment were insensitive to exogenous GA or PAC, especially the OsCSN1-deletion mutants, which were highly insensitive to PAC. Under GA treatment, the expression levels of phyB, CSN2, ABI5, and GID1 in the OsCSN1-deletion mutants increased, the expression levels of SLR1 and CUL1 decreased, and the expression level of PIL11 remained unchanged. The height of the OsCSN1-deletion mutants and mutant plants showed little change. Under PAC treatment, the expression level of GID1 increased; the expression levels of SLR1, ABI5, phyB, and CSN2 decreased; and the expression level of PIL11 decreased. OsCSN1-deletion mutants also showed the most significant increase in plant height.

These results showed that red light had a minor negative effect on the OsCSN1-deletion mutants, that exogenous GA did not aggravate the negative effect of red light, and that exogenous PAC did not inhibit the stem elongation of the mutants. It was speculated that OsCSN1 affected the activity of PIL11 by regulating the degradation of SLR1. The regulation of rice-stem elongation was caused by red light in rice: GID1 binds to GA to induce a conformational change in the GID1 protein. GID1 directly interacts with DELLA proteins to bind SLR1 to the ubiquitin E3 ligase complex (SCF SLY1/GID2), ultimately activating SLR1 via the 26S protease. Therefore, this enzyme can be degraded in the body to promote signal transduction by GA and regulate the height of rice plants.

OsCSN1-overexpressing plants exhibited enhanced sensitivity to red light. Under red-light treatment, plant height significantly increased, OsSLR1, OsABI5, OsphyB, and OsPIL11 expression levels significantly decreased, and OsCSN2, CUL1, and OsGID1 increased. Temporal and spatial locus data showed that a low level of GFP fusion protein was expressed in the leaves. Exogenous GA aggravated the sensitivity of OsCSN1 overexpression mutants to red light. Exogenous PAC inhibited the sensitivity of OsCSN1 overexpression mutants to red light but not completely. Under exogenous GA treatment, the expression levels of SLR1, ABI5, OsCSN2, CUL1, and phyB in the OsCSN1 overexpression mutants decreased, as did the expression level of PIL11. Temporal and spatial locus data showed that a high level of the GFP fusion protein was expressed in the leaves, and the amount in OsCSN1-overexpressing mutants also decreased. The expression mutants were sensitive to GA. Under exogenous PAC treatment, the expression levels of SLR1, ABI5, CSN2, CUL1, and PIL11 in OsCSN1-overexpressing plants increased, whereas the expression level of phyB decreased. A low level of the GFP fusion protein was expressed in the leaves of the spatiotemporal locus. These findings further suggested that OsCSN1 assembled into the CSN under red-light treatment, which degraded SLR1 through de-neddylation, affected PIL11 activity, and ultimately inhibited stem elongation.

4.3. Under Red Light, the Coleoptile Elongation of Rice Plants Is Affected by OsCSN1-Regulated PIL14 Degradation

The rice phytochromes phyA, phyB, and phyC play essential roles in plant photomorphogenesis. Light signals mediated by these three phytochromes inhibited the elongation of the coleoptile. phyB is the most essential red-light receptor [33]. In the presence of red light, phyB undergoes a conformational change from Pr to Pfr, which exposes the covered photoreceptor area, thereby causing the nuclear translocation of phyB. phyB also plays a significant role in inhibiting coleoptile elongation in seedlings under red light.

The expression of monochromatic red light had an inhibitory effect on rice coleoptiles and inhibited excessive elongation. The elongation of coleoptiles with OsCSN1 deletion

and reduced mutants was not sensitive to red light, and coleoptile elongation was not inhibited. OsSLR1, OsGID1, PIL14, and phyB levels increased. Under red-light treatment, PAC inhibited the elongation of coleoptiles in the OsCSN1 weak-expression mutants, but the difference was insignificant. However, PAC did not inhibit coleoptile elongation in OsCSN1-deletion mutants. Exogenous GA promoted the elongation of coleoptiles with OsCSN1 deletion and reduced the number of mutants.

Under red-light treatment, in the coleoptiles of OsCSN1 deletion and reduced mutants, although the expression levels of OsSLR1, OsGID1, and phyB increased, the expression level of PIL14 also increased. The degradation of PIL14 may require the ubiquitin/26S protease pathway regulated via OsCSN1. This conclusion is consistent with the fact that, under light conditions, photosensitized phyB in plant seedlings binds to PIF3 or PIF4, resulting in their ubiquitination.

The elongation of coleoptiles in OsCSN1-overexpressing plants is sensitive to red light, and the elongation of coleoptiles is inhibited by red light. The coleoptiles of the mutants expressed a high level of the GFP fusion protein; the expression levels of OsSLR1, OsGID1, and PIL14 were reduced, and the expression of phyB was reduced. The amount increased. Under red-light treatment, PAC inhibited the elongation of the coleoptiles of OsCSN1-overexpressing plants, did not express the GFP fusion protein, increased the expression levels of OsSLR1, OsGID1, and phyB, significantly decreased the expression level of PIL14, and inhibited the elongation of the coleoptiles. Exogenous GA rescued the inhibition of coleoptile elongation via red light in these mutants. A low level of the GFP fusion protein was expressed in the mutants; the expression levels of OsSLR1 and OsGID1 decreased, and the expression levels of phyB and PIL14 increased, promoting coleopsis and elongation. Under red-light treatment, OsCSN1-overexpressing plants formed CSN through CSN1 and regulated the degradation of SLR1 and PIL14 through the ubiquitin/26S protease pathway, ultimately affecting the elongation of the coleoptile.

Red light may regulate the degradation of SLR1 and PIL14 through the ubiquitin/26S protease pathway, eventually inhibiting the elongation of the coleoptile. OsCSN1 promotes the degradation of SLR1 and PIL14 by forming CSN and modifying it with RUB/NEDD8, an E3 ligase of CUL1 (Figure 5). This process eventually affects the elongation of coleoptiles.

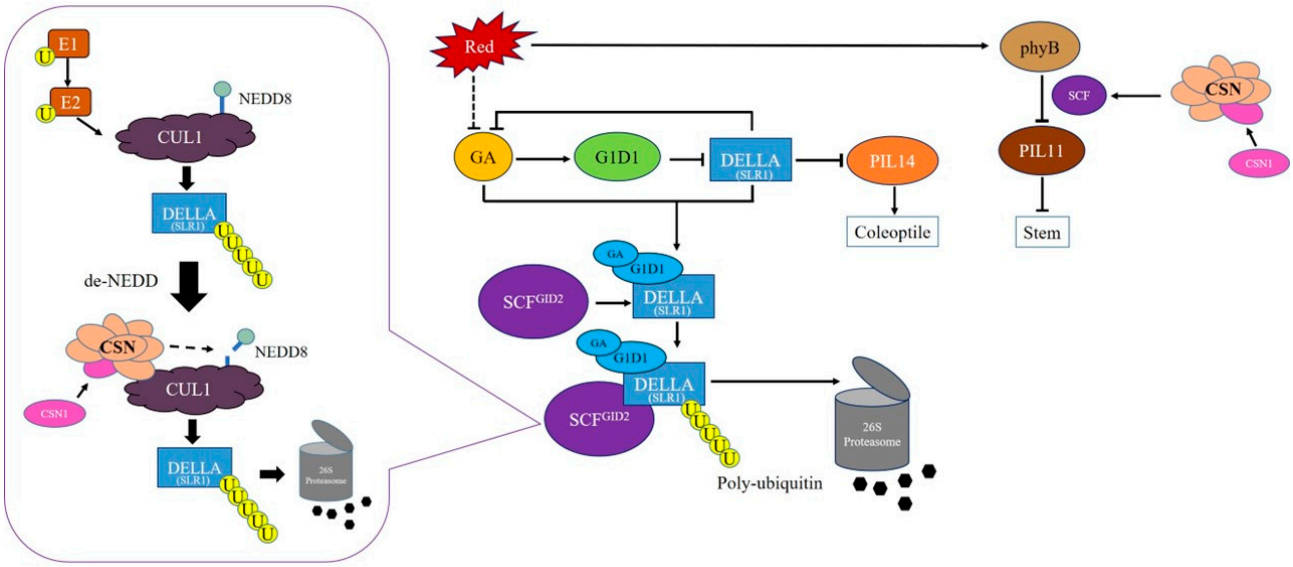

Figure 5. Presumed red light mediates the signaling pathway of OsCSN1 in regulating seedling growth and development.

Rice is one of the most important food crops in the world, and plant height is an important agronomic trait of rice. Plants that are too tall are prone to lodging, while those that are too short can lead to insufficient growth. Reducing plant height appropriately

without affecting other important agronomic traits is beneficial for increasing rice yield. Using molecular genetic methods and techniques to improve rice-plant height on the basis of existing excellent varieties is one of the effective ways to solve the problem of food security. In the research process of regulating the mechanism of rice-plant height, it has been found that there are many hormones that can regulate rice-plant height, and all of them can further affect rice yield. Therefore, understanding the regulatory mechanism and research progress of hormones on rice-plant height is of great significance for rice production and food security.

5. Conclusions

The research results indicate that OsCSN1 is a negative regulatory factor for red-light-regulated stem elongation in rice seedlings. Under red-light treatment, OsCSN1 is assembled into CSN, which undergoes NEDD acylation to degrade SLR1, affecting the PIL11 activity and ultimately inhibiting stem elongation. OsCSN1 also plays an important regulatory role in the inhibition of rice embryo sheath elongation under red light. By regulating the degradation of SLR1 and PIL14 through the ubiquitin/26S protease pathway, the elongation of the embryonic sheath is ultimately inhibited. OsCSN1 forms a COP9 complex and is modified with the RUB/NEDD8 of the E3 ligase of CUL1 to promote the degradation of SLR1 and PIL14, ultimately affecting the elongation of the embryonic sheath. The regulatory domain is located at the N-terminus of CSN1.

Supplementary Materials: The following supporting information can be downloaded at: https://www.mdpi.com/article/10.3390/agronomy14030572/s1, Figure S1. Laser confocal focusing on rice seedling leaves. Figure S2. Laser confocal focusing on rice root. Figure S3. Laser confocal focusing on rice coleoptile.

Author Contributions: S.H., M.W. and L.G. conceived and designed the experiments; S.H., T.J., L.Y., A.B. and H.Z. performed the experiments; S.H., W.Y., Y.L., M.X. and J.L. analyzed and discussed the data; S.H., M.W. and L.G. wrote and revised the article. All authors have read and agreed to the published version of the manuscript.

Funding: This study was funded by the Department of Jilin Province Science & Technology [grant numbers 20230203162SF, 20230402020GH, 20220402060GH, 20210203011SF, 20220203054SF].

Institutional Review Board Statement: Not applicable.

Informed Consent Statement: Not applicable.

Data Availability Statement: The data presented in this study are available in the article.

Acknowledgments: We thank the fundings from the Department of Jilin Province Science & Technology.

Conflicts of Interest: The authors declare no conflicts of interest.

References

1. Serino, G.; Deng, X.W. The COP9 signalosome: Regulating plant development through control of proteolysis. *Annu. Rev. Plant Biol.* **2003**, *54*, 165–182. [CrossRef] [PubMed]
2. Wei, N.; Deng, X.W. The COP9 signalosome. *Annu. Rev. Cell Dev. Biol.* **2003**, *19*, 261–286. [CrossRef] [PubMed]
3. Tuller, T.; Diament, A.; Yahalom, A.; Zemach, A.; Atar, S.; Chamovitz, D.A. The COP9 signalosome influences the epigenetic landscape of *Arabidopsis thaliana*. *Bioinformatics* **2019**, *35*, 2718–2723. [CrossRef] [PubMed]
4. Lyapina, S.; Cope, G.; Shevchenko, A.; Serino, G.; Tsuge, T.; Zhou, C.; Wolf, D.A.; Wei, N.; Shevchenko, A.; Deshaies, R.J. Promotion of NEDD-CUL1 conjugate cleavage by COP9 signalosome. *Science* **2001**, *292*, 1382–1385. [CrossRef]
5. Schwechheimer, C.; Serino, G.; Callis, J.; Crosby, W.L.; Lyapina, S.; Deshaies, R.J.; Gray, W.M.; Estelle, M.; Deng, X.W. Interactions of the COP9 signalosome with the E3 ubiquitin ligase SCFTIRI in mediating auxin response. *Science* **2001**, *292*, 1379–1382. [CrossRef] [PubMed]
6. Deshaies, R.J. SCF and Cullin/Ring H2-based ubiquitin ligases. *Annu. Rev. Cell Dev. Biol.* **1999**, *15*, 435–467. [CrossRef]
7. Hochstrasser, M. Evolution and function of ubiquitin-like protein-conjugation systems. *Nat. Cell Biol.* **2000**, *2*, E153–E157. [CrossRef]
8. Jentsch, S.; Pyrowolakis, G. Ubiquitin and its kin: How close are the family ties? *Trends Cell Biol.* **2000**, *10*, 335–342. [CrossRef]

9. Kawakami, T.; Chiba, T.; Suzuki, T.; Iwai, K.; Yamanaka, K.; Minato, N.; Suzuki, H.; Shimbara, N.; Hidaka, Y.; Osaka, F.; et al. NEDD8 recruits E2-ubiquitin to SCF E3 ligase. *EMBO J.* **2001**, *20*, 4003–4012. [CrossRef]
10. Franklin, K.A.; Quail, P.H. Phytochrome functions in Arabidopsis development. *J. Exp. Bot.* **2010**, *61*, 11–24. [CrossRef]
11. Gu, J.; Liu, J.; Xue, Y.; Zang, X.; Xie, X. Phytochrome functions in rice development. *Chin. J. Rice Sci.* **2011**, *25*, 130–135. [CrossRef]
12. Sharrock, R.A.; Quail, P.H. Novel phytochrome sequences in *Arabidopsis thaliana*: Structure, evolution, and differential expression of a plant regulatory photoreceptor family. *Genes Dev.* **1989**, *3*, 1745–1757. [CrossRef]
13. Clack, T.; Mathews, S.; Sharrock, R.A. The phytochrome apoprotein family in Arabidopsis is encoded by five genes: The sequences and expression of PHYD and PHYE. *Plant Mol. Biol.* **1994**, *25*, 413–427. [CrossRef]
14. Kay, S.A.; Keith, B.; Shinozaki, K.; Chua, N.H. The sequence of the rice phytochrome gene. *Nucleic Acids Res.* **1989**, *17*, 2865–2866. [CrossRef]
15. Dehesh, K.; Tepperman, J.; Christensen, A.H.; Quail, P.H. phyB is evolutionarily conserved and constitutively expressed in rice seedling shoots. *Mol. Genet. Genom.* **1991**, *225*, 305–313. [CrossRef]
16. Tahir, M. Phytochrome C (PHYC) gene in rice: Isolation and characterization of a complete coding sequence. *J. Plant Physiol.* **1998**, *118*, 1535. [CrossRef]
17. Basu, D.; Dehesh, K.; Schneider-Poetsch, H.J.; Harrington, S.E.; McCouch, S.R.; Quail, P.H. Rice PHYC gene: Structure, expression, map position and evolution. *Plant Mol. Biol.* **2000**, *44*, 27–42. [CrossRef]
18. Hamdani, S.; Khan, N.; Perveen, S.; Qu, M.; Jiang, J.; Zhu, X.G. Changes in the photosynthesis properties and photoprotection capacity in rice (*Oryza sativa*) grown under red, blue, or white light. *Photosynth. Res.* **2019**, *139*, 107–121. [CrossRef]
19. Muneer, S.; Kim, E.J.; Park, J.S.; Lee, J.H. Influence of green, red and blue light emitting diodes on multiprotein complex proteins and photosynthetic activity under different light intensities in lettuce leaves (*Lactuca sativa* L.). *Int. J. Mol. Sci.* **2014**, *15*, 4657–4670. [CrossRef]
20. Hogewoning, R.; Kubota, C. Physiological responses of cucumber seedlings under different blue and red photon flux ratios using LEDs. *Environ. Exp. Bot.* **2016**, *121*, 66–74. [CrossRef]
21. Quail, P.H. Phytochrome photosensory signalling networks. *Nat. Rev. Mol. Cell Biol.* **2002**, *3*, 85–93. [CrossRef] [PubMed]
22. Rockwell, N.C.; Su, Y.S.; Lagarias, J.C. Phytochome structure and signaling mechanisms. *Annu. Rev. Plant Biol.* **2006**, *57*, 837–858. [CrossRef]
23. Hoenecke, M.E.; Bula, R.J.; Tibbitts, T.W. Importance of Blue'Photon Levels for Lettuce Seedlings Grown under Red-light-emitting Diodes. *HortScience* **1992**, *27*, 427–430. [CrossRef]
24. Miao, Y.X.; Wang, X.Z.; Gao, L.H.; Chen, Q.Y.; Mei, Q.U. Blue light is more essential than red light for maintaining the activities of photosystem II and I and photosynthetic electron transport capacity in cucumber leaves. *J. Integr. Agric.* **2016**, *15*, 87–100. [CrossRef]
25. Goins, G.D.; Yorio, N.C.; Sanwo, M.M.; Brown, C.S. Photomorphogenesis, photosynthesis, and seed yield of wheat plants grown under red light-emitting diodes (LEDs) with and without supplemental blue lighting. *J. Exp. Bot.* **1997**, *48*, 1407–1413. [CrossRef]
26. Sæbø, A.; Krekling, T.; Appelgren, M. Light quality affects photosynthesis and leaf anatomy of birch plantlets in vitro. *Plant Cell Tissue Organ Cult.* **1995**, *41*, 177–185. [CrossRef]
27. Su, N.; Wu, Q.; Shen, Z.; Xia, K.; Cui, J. Effects of light quality on the chloroplastic ultrastructure and photosynthetic characteristics of cucumber seedlings. *Plant Growth Regul.* **2014**, *73*, 227–235. [CrossRef]
28. Trouwborst, G.; Hogewoning, S.W.; van Kooten, O.; Harbinson, J.; van Ieperen, W. Plasticity of photosynthesis after the 'red light syndrome'in cucumber. *Environ. Exp. Bot.* **2016**, *121*, 75–82. [CrossRef]
29. Darko, E.; Heydarizadeh, P.; Schoefs, B.; Sabzalian, M.R. Photosynthesis under artificial light: The shift in primary and secondary metabolism. *Philos. Trans. R. Soc. B Biol. Sci.* **2014**, *369*, 20130243. [CrossRef]
30. Hogewoning, S.W.; Trouwborst, G.; Maljaars, H.; Poorter, H.; van Ieperen, W.; Harbinson, J. Blue light dose-responses of leaf photosynthesis, morphology, and chemical composition of Cucumis sativus. *J. Exp. Bot.* **2010**, *61*, 3107–3117. [CrossRef]
31. Chen, C.C.; Huang, M.Y.; Lin, K.H.; Wong, S.L.; Huang, W.D.; Yang, C.M. Effects of light quality on the growth, development and metabolism of rice seedlings (*Oryza sativa* L.). *J. Biotechnol.* **2014**, *9*, 15–24. [CrossRef]
32. Adams, W.W.; Muller, O.; Cohu, C.M.; Demmig-Adams, B. May photoinhibition be a consequence, rather than a cause, of limited plant productivity? *Photosynth. Res.* **2013**, *117*, 31–44. [CrossRef]
33. Chen, M.; Tao, Y.; Lim, J.; Shaw, A.; Chory, J. Regulation of phytochrome B nuclear localization through light-dependent unmasking of nuclear-localization signals. *Curr. Biol.* **2005**, *15*, 637–642. [CrossRef]
34. Xie, X.; Shinomura, T.; Inagaki, N.; Kiyota, S.; Takano, M. Phytochrome-mediated inhibition of coleoptile growth in rice: Age-dependency and action spectra. *Photochem. Photobiol.* **2007**, *83*, 131–138. [CrossRef]
35. Cho, J.N.; Ryu, J.Y.; Jeong, Y.M.; Park, J.; Song, J.J.; Amasino, R.M.; Noh, Y.S. Control of seed germination by light-induced histone arginine demethylation activity. *Dev. Cell* **2012**, *22*, 736–748. [CrossRef] [PubMed]
36. Kim, S.T.; Kang, S.Y.; Wang, Y.; Kim, S.G.; Hwang, D.H.; Kang, K.Y. Analysis of embryonic proteome modulation by GA and ABA from germinating rice seeds. *Proteomics* **2008**, *8*, 3577–3587. [CrossRef]
37. Hornitschek, P.; Kohnen, M.V.; Lorrain, S.; Rougemont, J.; Ljung, K.; López-Vidriero, I.; Fankhauser, C. Phytochrome interacting factors 4 and 5 control seedling growth in changing light conditions by directly controlling auxin signaling. *Plant J.* **2012**, *71*, 699–711. [CrossRef]

38. Fleet, C.M.; Sun, T.P. A DELLA cate balance: The role of gibberellin in plant morphogenesis. *Curr. Opin. Plant Biol.* **2005**, *8*, 77–85. [CrossRef]
39. Lange, M.P.; Lange, T. Gibberellin biosynthesis and the regulation of plant development. *Plant Biol.* **2006**, *8*, 281–290. [CrossRef]
40. Hauvermale, A.L.; Ariizumi, T.; Steber, C.M. Gibberellin signaling: A theme and variations on DELLA repression. *Plant Physiol.* **2012**, *160*, 83–92. [CrossRef] [PubMed]
41. Dai, C.; Xue, H.W. Rice early flowering1, a CKI, phosphorylates DELLA protein SLR1 to negatively regulate gibberellin signalling. *EMBO J.* **2010**, *29*, 1916–1927. [CrossRef] [PubMed]
42. Ariizumi, T.; Hauvermale, A.L.; Nelson, S.K.; Hanada, A.; Yamaguchi, S.; Steber, C.M. Lifting della repression of Arabidopsis seed germination by nonproteolytic gibberellin signaling. *Plant Physiol.* **2013**, *162*, 2125–2139. [CrossRef] [PubMed]
43. Huq, E.; Al-Sady, B.; Quail, P.H. Nuclear translocation of the photoreceptor phytochrome B is necessary for its biological function in seed-ling photomorphogenesis. *Plant J.* **2003**, *35*, 660–664. [CrossRef] [PubMed]
44. Chen, M.; Chory, J.; Fankhauser, C. Light signal transduction in higher plants. *Annu. Rev. Genet.* **2004**, *38*, 87–117. [CrossRef] [PubMed]
45. Castillon, A.; Shen, H.; Huq, E. Phytochrome interacting factors: Central players in phytochrome-mediated light signaling networks. *Trends Plant Sci.* **2007**, *12*, 514–521. [CrossRef] [PubMed]
46. Feng, S.; Martinez, C.; Gusmaroli, G.; Wang, Y.; Zhou, J.; Wang, F.; Chen, L.; Yu, L.; Iglesias-Pedraz, J.M.; Kircher, S.; et al. Coordinated regulation of *Arabidopsis thaliana* development by light and gibberellins. *Nature* **2008**, *451*, 475–479. [CrossRef] [PubMed]
47. De Lucas, M.; Davière, J.M. Rodríguez-Falcón M; et al. A molecular framework for light and gibberellin control of cell elongation. *Nature* **2008**, *451*, 480–484. [CrossRef]
48. Leivar, P.; Quail, P.H. PIFs: Pivotal components in a cellular signaling hub. *Trends Plant Sci.* **2011**, *16*, 19–28. [CrossRef]
49. Lu, X.D.; Zhou, C.M.; Xu, P.B.; Luo, Q.; Lian, H.L.; Yang, H.Q. Red-light-dependent interaction of phyB with SPA1 promotes COP1-SPA1 dissociation and photomorphogenic development in Arabidopsis. *Mol. Plant* **2015**, *8*, 467–478. [CrossRef]
50. Alabadí, D.; Gil, J.; Blázquez, M.A.; García-Martínez, J.L. Gibberellins repress photomorphogenesis in darkness. *Plant Physiol.* **2004**, *134*, 1050–1057. [CrossRef]
51. Matsushita, T.; Mochizuki, N.; Nagatani, A. Dimers of the N-terminal domain of phytochrome B are functional in the nucleus. *Nature* **2003**, *424*, 571–574. [CrossRef] [PubMed]
52. Ni, M.; Teppeman, J.M.; Quail, P.H. PIF3, a phytochrome-interacting factor necessary for normal photoinduced signal transduction, is a novel basic helix-loop-helix protein. *Cell* **1998**, *95*, 657–667. [CrossRef]
53. Huq, E.; Quail, P.H. PIF4, a phytochrome-interacting bHLH factor, functions as a negative regulat or of phytochrome B signaling in Arabidopsis. *EMBO J.* **2002**, *21*, 2441–2450. [CrossRef]
54. Shen, Y.; Khanna, R.; Carle, C.M.; Quail, P.H. Phytochrome induces rapid PIF5 phosphorylation and degradation in response to red-light activation. *Plant Physiol.* **2007**, *145*, 1043. [CrossRef] [PubMed]
55. Tsutomu, I.; Masayuki, H.; Yukari, H.; Motoaki, S.; Masatomo, K.; Tomohiko, K.; Satoshi, T.; Kazuo, S.; Tatsuo, K. Identification of CREl as a cytokinin receptor from Arabidopsis. *Nature* **2001**, *409*, 1060–1063. [CrossRef]
56. Lee, N.; Choi, G. Phytochrome-interacting factor from Arabidopsis, to liverwort. *Curr. Opin. Plant Biol.* **2017**, *35*, 54–60. [CrossRef]